GREEN BIOSYNTHESIS OF SnO_2 NANOPARTICLES BY *PLECTRANTHUS AMBOINICUS* LEAF EXTRACT THEIR PHOTOCATALYTIC ACTIVITY TOWARD RHODAMINE B DEGRADATION

L. FU[a,b], Y. ZHENG[a*], Q. REN[a], A. WANG[c], B. DENG[d]
[a]*Institute of Botany, Jiangsu Province and Chinese Academy of Sciences, Nanjing Botanical Garden, Mem. Sun Yat-Sen, Nanjing 210014, China*
[b]*Golden Yuanta Construction Engineering Co., Ltd, Zhejiang 311200, China*
[c]*Department of Physics and Materials Science, City University of Hong Kong, Hong Kong*
[d]*Jiangsu Junma Park Technology Co. Ltd, Jiangsu, China*

In this paper, we report the first time preparation of SnO_2 nanoparticles (NPs) using a green chemistry method. The leaf extract of *Plectranthus amboinicus* was used as reducing and stabilization agent for synthesizing SnO_2 NPs. The synthesized SnO_2 NPs were characterized by SEM, EDX, XRD and UV-vis spectroscopy. Results showed that the biosynthesized SnO_2 NPs owing a high purity. The photocatalytic property of the biosynthesized SnO_2 NPs was investigated by photodegradation of rhodamine B (Rh B) under visible light illumination. Results indicated that the photocatalytic performance of the biosynthesized SnO_2 NPs is much higher than that of commercial SnO_2. Moreover, the biosynthesized SnO_2 also exhibited an excellent reusability.

(Receved November 30, 2014; Accepted January 8, 2014)

Keyword: Biosynthesis; SnO_2 nanoparticles; *Plectranthus amboinicus*; Photodegradation; Rhodamine B

1. Introduction

Numerous efforts have been made to development of semiconductor nanoparticles (NPs) in the last two decades due to their novel optical, chemical, photo-electrochemical and electronic properties which are different from that of bulk. Stannic oxide (SnO_2) is a well know n-type wide-bandgap (Eg = 3.6 eV) semiconductor. Nano-sized SnO_2 is regarded as a highly preferred multitasking metal oxide, such as gas sensors and lithium rechargeable batteries [1-13]. SnO_2 NPs are commonly synthesized by wet chemical route [14, 15], vapor phase process [16, 17], hydrothermal method [18-20], precipitation [21, 22], electrodeposition and sonochemical method [23-25]. However, chemical methods lead to the presence of some toxic chemicals adsorbed on the surface that may have adverse effects in applications and environment. Thus, to design a simple and green route to synthesize SnO_2 NPs is of considerable necessary.

Recently, development of an eco-friendly method for the synthesis of nanoparticles via biological methods has been attracted lots of attentions. Using bacterial, fungi and plant extract are three main routes for biosynthesis of nanomaterials. For example, Singh et al. [26] reported the synthesis of ZnO NPs using the cell extract of the cyanobacterium, *Anabaen*a strain L31. Jain and co-workers reported the preparation of ZnO NPs using the extracellular fungal proteins [27]. Jayaseelan et al. [28] demonstrated the synthesis of Au NPs using seed aqueous extract of *Abelmoschus esculentus*. Among them, synthesis of nanomaterials using plant extract attracted lots attention by researchers due to its lower cost and simplicity. To the authors' best knowledge and review of the literature, the biosynthesis of SnO_2 only conducted by using bacterium *Erwinia herbicola* as reducing agent [29].

* Corresponding author: yuhongzhengcas@gmail.com

Plectranthus amboinicus is a tender fleshy perennial plant in the family Lamiaceae with an oregano-like flavor and odor. The biogenic synthesis performance of *Plectranthus amboinicus* has been tested by Ajitha et al. [30]. They reported the utilization of *Plectranthus amboinicus* leaf extract as reducing agent for synthesizing Ag NPs. The synthesized Ag NPs exhibited an excellent antimicrobial property. Herein, we report for the first time synthesis of SnO_2 NPs using *Plectranthus amboinicus* leaf extract as reducing agent. A series of techniques have been used for characterizing biosynthesized SnO_2 NPs. The photocatalytic activity of biosynthesized SnO_2 NPs was then evaluated by photodegradation of RhB under visible light.

2. Experimental

2.1 Materials

Plectranthus amboinicus plants were purchased from a local nursery of Zhejiang province, China. The plant was taxonomically identified and authenticated by the botanical survey of Hangzhou botanical garden. The plant leaves were cleaned with double distilled water. Then, 5 g of *Plectranthus amboinicus* leaves were washed with water and cut into small pieces. The leaf extract was obtained sonication of leaves for 1 h. Then, the extract was collected, filtered through Whatman No. 1 filter paper and stored in refrigerator for further experiments. Tin(II) chloride dehydrate ($SnCl_2 \cdot 2H_2O$) and rhodamine B (Rh B) were purchased from Sigma-Aldrich. All other chemicals used were analytical grade reagents without further purification.

2.2 Biosynthesis of SnO_2 NPs

For synthesis of SnO_2 NPs, 0.5 M zinc nitrate solution was prepared with 30 mL water. Then 20 mL *Plectranthus amboinicus* leaf extract was added to above solution and stirring for 10 min. Afterward, 0.5 mL H_2SO_4 (5 M) was added into the above dispersion. The suspension was transferred to 50 mL Teflon-lined stainless steel autoclave. The autoclave was heated to 200°C and maintained for 3 h in an oven and naturally cooled down to the room temperature. The sediments were centrifuged, washed with water, and calcined at 300°C for 2 h to result SnO_2.

2.3 Characterization of the synthesized SnO_2 NPs

The morphology of as-synthesized SnO_2 NPs was observed using a ZEISS, SUPRA 55 field emission scanning electron microscopy (FESEM) measurements. The particle size of the biosynthesized SnO_2 NPs was measured using a particle size analyzer (SALD-7500nano, SHIMADZU). The crystal phase information of sample was characterized from 20° to 80° in 2θ by a XRD with Cu Kα (λ = 0.1546 nm).radiation (D8-Advanced, Bruker). The optical analysis was obtained by UV-vis spectrophotometer (Perkin Elmer Lambda 950).

2.4 Photocatalytic activity evaluation

The photocatalytic activity of the biologically synthesized SnO_2 NPs and commercial SnO_2 was compared by degradation of RhB in aqueous solution as a model system. The visible light used in the present study was obtained using the filter with cut-off wavelength of 420 nm. In a typical photodegradation process, 20 mg sample was added to 10 ml of RhB (20 mg/L) solution. The absorbance spectrum of the solution was monitored using UV-Vis spectrophotometer at wavelength 553 nm at different time intervals.

3. Results and discussion

The morphology of biosynthesized SnO_2 NPs was observed by SEM. Figure 1 shows the SEM images of SnO_2 NPs at different magnifications. It can be seen that the formed SnO_2 NPs

show a cluster structure. Due to the aggregation, the individual size of the biosynthesized SnO_2 cannot be measured visually. The particle size analyzer indicated the average size of the biosynthesized SnO_2 NPs is 63 nm.

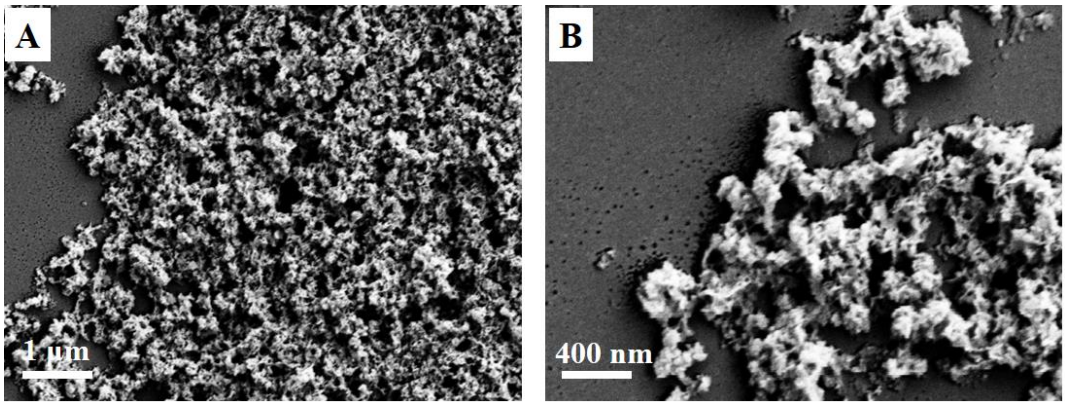

Fig. 1: SEM images of biosynthesized SnO_2 at (A) low and (B) high magnification.

Fig. 2A displays the EDX spectrum of biosynthesized SnO_2 NPs, which confirmed the presence of elemental stannum and oxygen signals. No other impurity element was observed in the sample, indicating the high purity of the biosynthesized SnO_2 after calcination process. Therefore, using *Plectranthus amboinicus* leaf extract for SnO_2 synthesis is a reliable method.

The crystal structure of the biosynthesized SnO_2 NPs was characterized by XRD. Figure 2B represents the XRD pattern of biosynthesized SnO_2 NPs, which displays various well-defined diffraction peaks. It can be observed that the diffraction peaks at 26.75°, 37.88°, 39.35°, 51.95°, 54.50°, 57.93°, 62.09°, 64.95°, 66.08°, 69.32°, 71.70° and 79.13° can be indexed to (110), (200), (111), (211), (220), (002), (310), (112), (301), (202) and (321) crystal planes of tetragonal SnO_2 (JCPDS card No. 41-1445). It is worth noting that the diffraction peaks related to any impurities were not observed, further indicating the proposed biosynthesis route could be applied for high purity SnO_2 NPs production.

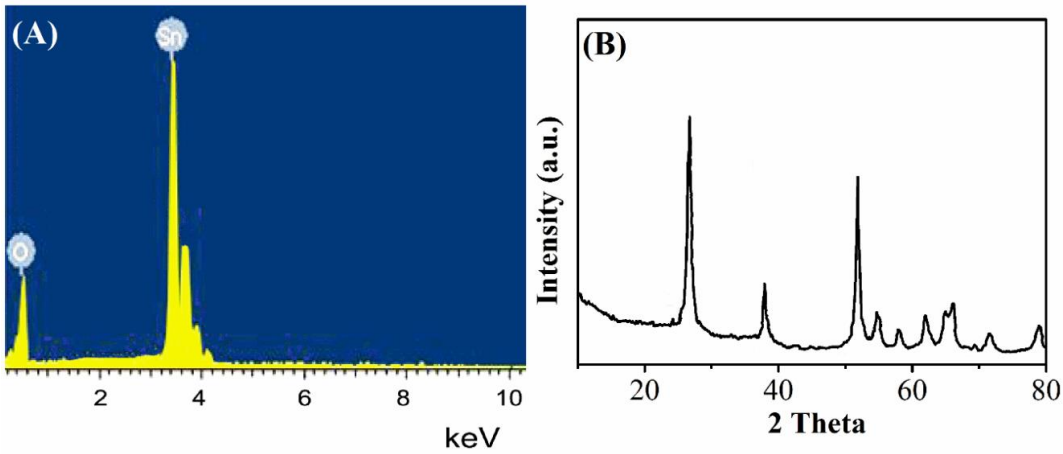

Fig. 2. (A) EDX spectrum and (B) XRD pattern of biosynthesized SnO_2 NPs.

The light absorbance properties of biosynthesized SnO_2 NPs were investigated using UV-vis spectroscopy and its disuse reflectance. Figure 3A shows the diffuse absorption spectra of commercial SnO_2 and biosynthesized SnO_2 NPs. It can be clearly observed that the biosynthesized SnO_2 NPs exhibit a higher absorbance than commercial SnO_2. From the reflectance spectrum of SnO_2 NPs (Figure 3B), we also can observe a high light reflectance, which light could result in a

high rate of light harvesting [31]. The high absorbance and scattering of the SnO_2 NPs can increase the number of photo-generated electrons and holes to involve in the photocatalytic reaction and enhance the photocatalytic performance [32].

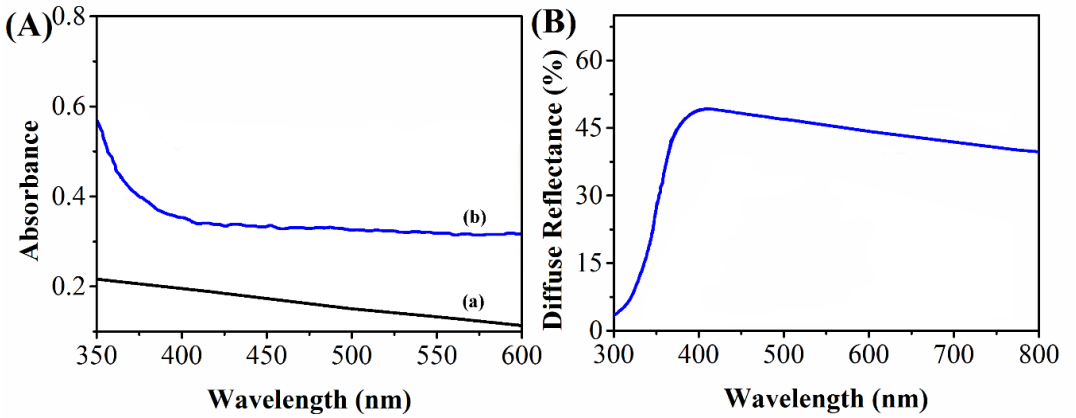

Fig. 3. (A) UV-vis diffuse absorption spectra of commercial SnO_2 (a) and biosynthesized SnO_2 NPs (b). (B) UV-vis diffuse reflectance spectrum of biosynthesized SnO_2 NPs.

The photocatalytic activity of the biosynthesized SnO_2 NPs was investigated by photodegradation of RhB, and compared with commercial SnO_2. The Langmuir and Hinshelwood models [33] were adopted for explaining the relationship between the photodegradation rate in the presence of SnO_2 NPs with respect to time. The rate equation can be express as:

$$\frac{-dC}{dt} = \frac{k_{L\text{-}H}K_{ad}C}{1+K_{ad}C'}$$

Where K_{ad} is the adsorption coefficient of the reaction on SnO_2 NPs, $k_{L\text{-}H}$ is the reaction rate constant and C is the concentration at any time t.

$$Ln(C_0/C) = K(C\text{-}C_0) + k_{L\text{-}H}K_{ad}t$$

Where C_0 is the initial concentration. Because the $K_{ad}C$ is very small, Thus it can be simplified and integrated as:

$$Ln(C_0/C) = k_{L\text{-}H}K_{ad}t = kt$$

Where $k = k_{L\text{-}H}K_{ad}$ is the first order reaction rate constant.

The photodegradation profiles of different photocatalysts are shown in Figure 4A. A control experiment was firstly performed without adding any catalyst in Rh B solution to check if any degradation appears under visible irradiation. The small decreasing of the concentration with time was attributed to the occurrence of cleavage in the aromatic ring of the RhB molecules. It was observed that the Rh B concentration had decreased by about 5.3 % after 120 min irradiation. While the photodegradation rate of commercial SnO_2 was 42.7% after 120 min visible light irradiation. In contrast, the biosynthesized SnO_2 NPs displayed a much higher performance, which could degrade more than 95% of RhB in after 120 min light illumination. The photocatalytic degradation of RhB using SnO_2 can be explained as follow: the conduction band electrons and the valence band holes are firstly generated when the SnO_2 NPs are illuminated by light. OH^- radicals are produced on the hydroxyl group at the SnO_2 when the holes are trapped on the surface. While, the superoxide radical anions O_2^- are produced when the reaction of dissolved oxygen molecule with electrons. Then, the superoxide radical anions O_2^- can produce hydroxyl radicals, HO_2 by

protonation. Finally, the RhB molecules are degraded by these radicals [34-38]. The superior photocatalytic activity of the biosynthesized SnO_2 NPs could ascribe to their high specific surface area, which provides maximum exposure for reactant to the active site [29].

Fig. 4B shows the first-order kinetic linear curves of different photocatalysts. The apparent rate constant of commercial SnO_2 and biosynthesized SnO_2 NPs can be calculated to be 0.0015 and 0.0121/min, respectively. The reusability of the biosynthesized SnO_2 was also investigated. After 5 cycles test, the biosynthesized SnO_2 NPs remain more than 91% of photodegradation performance, suggesting that the proposed photocatalyst owing an excellent stability.

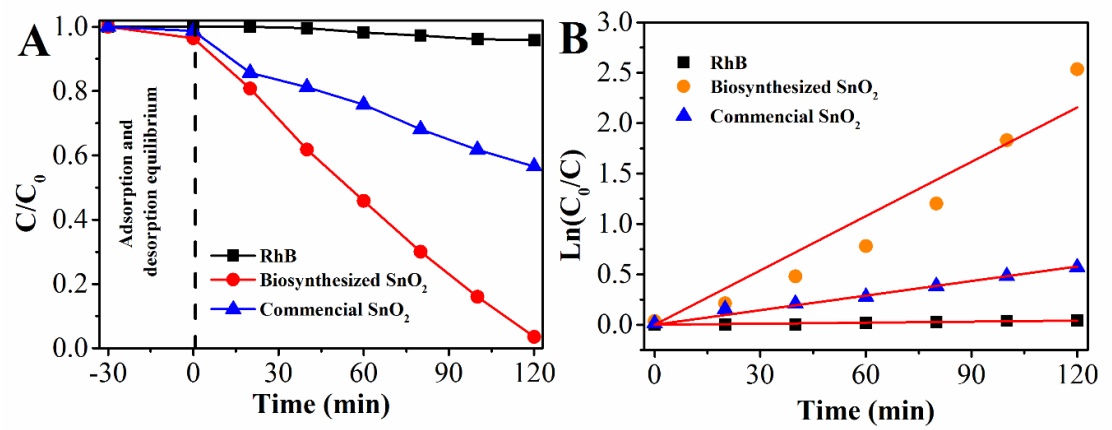

Fig. 4: (A) Comparison of RhB photodegradation in the absence and presence of different photocatalysts under visible light irradiation. (B) The first-order kinetic model fit for different photocatalysts.

4. Conclusion

In summary, *Plectranthus amboinicus* assisted synthesis of SnO_2 NPs was achieved using a simple one-pot hydrothermal approach. The average size of synthesized SnO_2 NPs was determined as 63 nm. EDX and XRD characterizations suggest the proposed biosynthesis method could results high purity of SnO_2 NPs. Moreover, the proposed biosynthesis method has advantages over the other methods, such as ease with the process which can be scaled up and economic viability. Moreover, the biosynthesized SnO_2 NPs showed a superior photocatalytic performance towards dye molecules degradation.

Acknowledgments

Authors acknowledge financial support from National Natural Science Foundation of Jiangsu Province (Grant no BE2013625) and Jiangsu Planned Projects for Postdoctoral Research Funds (1402126C).

Reference

[1] B.W. Hwang, S.C. Lee, S.Y. Kim, S.Y. Jung, B.H. Park, J.H. Kim, I.S. Son, J.S. Huh, D.D. Lee, J.C. Kim, Sensor Letters **12,** 1080 (2014).
[2] D. Xiang, H. Lin, L. Li, X. Chen, J. Ma, F. Qu, Materials Focus **3,** 325 (2014).
[3] H. Cai, B. Liu, Q.A. Qiao, Z. Lin, Journal of Computational and Theoretical Nanoscience **6,** 701 (2014).
[4] A. Singh, A. Sharma, M. Tomar, V. Gupta, Advanced Science Letters **20,** 1056 (2014).
[5] K. Wang, Y. Huang, H. Huang, M. Zong, J. Ding, Y. Wang, Mater. Technol. 1753555714Y.0000000184 (2014).

[6] M.V. Reddy, L. Yu Tse, W.K.Z. Bruce, B.V.R. Chowdari, Materials Letters **138,** 231 (2015).
[7] Y. Liu, K. Xie, Science of Advanced Materials **6,** 863 (2014).
[8] M.Z. Iqbal, F. Wang, R. Hussain, T. Iqbal, I. Ali, M.Y. Rafique, S. Ali, Advanced Science, Engineering and Medicine **6,** 791 (2014).
[9] S. Zhang, W. He, X. Zhang, J. Ma, C. Sun, X. Song, Energy and Environment Focus **3,** 320 (2014).
[10] U.E. Uno, M.E. Emetere, M. Aplha, Journal of Ovonic Research **10,** 83 (2014).
[11] E.F. Keskenler, G. Turgut, S. Aydin, R. Dilber, U. Turgut, Journal of Ovonic Research **9,** 61 (2013).
[12] A. Kocyigit, D. Tatar, A. Battal, M. Ertugrul, B. Duzgun, Journal of Ovonic Research **8,** 171 (2012).
[13] A.M. Ungureanu, C. Andronescu, G. Voicu, A. Scoban, O. Oprea, N. Stanica, I. Jitaru, Digest Journal of Nanomaterials and Biostructures **8,** 1169 (2013).
[14] Q. Guo, X. Qin, Journal of Solid State Electrochemistry **18,** 1031 (2014).
[15] X. Wang, S. Qiu, J. Liu, C. He, G. Lu, W. Liu, European Journal of Inorganic Chemistry **2014,** 863 (2014).
[16] J.M. Roller, H. Yu, L. Zhang, P. Plachinda, M.B. Vukmirovic, S. Bliznakov, M. Li, R.R. Adzic, R. Maric, Microscopy and Microanalysis **20,** 462 (2014).
[17] Y.-C. Her, B.-Y. Yeh, S.-L. Huang, ACS applied materials & interfaces **6,** 9150 (2014).
[18] X. Wang, C. Zhao, R. Liu, Q. Shen, Journal of Nanoparticle Research **16,** 1 (2014).
[19] R.K. Mishra, A. Kushwaha, P.P. Sahay, Journal of Experimental Nanoscience 1 (2014).
[20] A. Amutha, B.K. Panigrahi, S. Amirthapanian, P. Thangadurai, AIP Conference Proceedings **1591,** 577 (2014).
[21] N. Yongvanich, S. Maensiri, Integrated Ferroelectrics **156,** 53 (2014).
[22] R. Noonuruk, N. Vittayakorn, W. Mekprasart, J. Sritharathikhun, W. Pecharapa, Journal of Nanoscience and Nanotechnology **15,** 2564 (2015).
[23] D.V. Raj, N. Ponpandian, D. Mangalaraj, A. Balamurugan, C. Viswanathan, Ionics **20,** 335 (2014).
[24] S.M. Mirali, K. Jafarzadeh, M. Mirjani, Transactions of the IMF 0020296714Z.000000000185 (2014).
[25] V. Sahu, S. Lalwani, G. Singh, R.K. Sharma, Advanced Science Letters **20,** 1369 (2014).
[26] G. Singh, P.K. Babele, A. Kumar, A. Srivastava, R.P. Sinha, M.B. Tyagi, Journal of photochemistry and photobiology. B, Biology **138,** 55 (2014).
[27] N. Jain, A. Bhargava, J. Panwar, Chemical Engineering Journal **243,** 549 (2014).
[28] C. Jayaseelan, R. Ramkumar, A.A. Rahuman, P. Perumal, Industrial Crops and Products **45,** 423 (2013).
[29] N. Srivastava, M. Mukhopadhyay, Industrial & Engineering Chemistry Research **53,** 13971 (2014).
[30] B. Ajitha, Y. Ashok Kumar Reddy, P. Sreedhara Reddy, Spectrochimica Acta Part A: Molecular and Biomolecular Spectroscopy **128,** 257 (2014).
[31] X. Liu, L. Pan, T. Chen, J. Li, K. Yu, Z. Sun, C. Sun, Catalysis Science & Technology **3,** 1805 (2013).
[32] T. Xu, L. Zhang, H. Cheng, Y. Zhu, Appl Ctatl B-Environ **101,** 382 (2011).
[33] A. Houas, H. Lachheb, M. Ksibi, E. Elaloui, C. Guillard, J.-M. Herrmann, Appl Ctatl B-Environ **31,** 145 (2001).
[34] Z. Tian, C. Liang, J. Liu, H. Zhang, L. Zhang, Journal of Materials Chemistry **21,** 18242 (2011).
[35] J.S. Lee, O.S. Kwon, J. Jang, Journal of Materials Chemistry **22,** 14565 (2012).
[36] M.M. Rashad, A.A. Ismail, I. Osama, I.A. Ibrahim, A.-H.T. Kandil, CLEAN – Soil, Air, Water **42,** 657 (2014).
[37] Q. Luo, Q.Z. Cai, J. He, X.W. Li, X.D. Chen, Advances in Applied Ceramics **113,** 228 (2014).
[38] W. Yu, Q. Ma, C. Wang, X. Dong, J. Wang, G. Liu, Materials Express **4,** 435 (2014).